(4)

AD-A200 326

RADC-TR-88-121
In-House Report
May 1988

A WIDE-BAND PRINTED CIRCUIT DIPOLE

Paul M. Proudfoot, 2Lt, USAF

APPROVED FOR PUBLIC RELEASE; DISTRIBUTION UNLIMITED.

ROME AIR DEVELOPMENT CENTER
Air Force Systems Command
Griffiss AFB, NY 13441-5700

This report has been reviewed by the RADC Public Affairs Office (PA) and is releasable to the National Technical Information Service (NTIS). At NTIS it will be releasable to the general public, including foreign nations.

RADC-TR-88-121 has been reviewed and is approved for publication.

APPROVED:

ROBERT J. MAILLOUX
Acting Chief, Antennas & Components Division
Directorate of Electromagnetics

APPROVED:

JOHN K. SCHINDLER
Acting Director of Electromagnetics

FOR THE COMMANDER:

JOHN A. RITZ
Directorate of Plans & Programs

If your address has changed or if you wish to be removed from the RADC mailing list, or if the addressee is no longer employed by your organization, please notify RADC (EEAA) Hanscom AFB MA 01731-5000. This will assist us in maintaining a current mailing list.

Do not return copies of this report unless contractual obligations or notices on a specific document require that it be returned.

UNCLASSIFIED

SECURITY CLASSIFICATION OF THIS PAGE

REPORT DOCUMENTATION PAGE

1a. REPORT SECURITY CLASSIFICATION Unclassified	1b. RESTRICTIVE MARKINGS
2a. SECURITY CLASSIFICATION AUTHORITY	3. DISTRIBUTION/AVAILABILITY OF REPORT Approved for public release; distribution unlimited.
2b. DECLASSIFICATION/DOWNGRADING SCHEDULE	
4. PERFORMING ORGANIZATION REPORT NUMBER(S) RADC-TR-88-121	5. MONITORING ORGANIZATION REPORT NUMBER(S)
6a. NAME OF PERFORMING ORGANIZATION Rome Air Development Center 6b. OFFICE SYMBOL (If applicable) EEAA	7a. NAME OF MONITORING ORGANIZATION
6c. ADDRESS (City, State, and ZIP Code) Hanscom Air Force Base Massachusetts, 01731-5000	7b. ADDRESS (City, State, and ZIP Code)
8a. NAME OF FUNDING/SPONSORING ORGANIZATION Rome Air Development Center 8b. OFFICE SYMBOL (If applicable)	9. PROCUREMENT INSTRUMENT IDENTIFICATION NUMBER
8c. ADDRESS (City, State, and ZIP Code) Hanscom Air Force Base Massachusetts, 01731-5000	10. SOURCE OF FUNDING NUMBERS PROGRAM ELEMENT NO. 62702F; PROJECT NO. 4600; TASK NO. 14; WORK UNIT ACCESSION NO. 02

11. TITLE (Include Security Classification)

A Wide-Band Printed Circuit Dipole

12. PERSONAL AUTHOR(S)

Proudfoot, Paul M., 2Lt, USAF

13a. TYPE OF REPORT	13b. TIME COVERED	14. DATE OF REPORT (Year, Month, Day)	15. PAGE COUNT
In-House	FROM Jul 87 TO Mar 88	1988 May	

16. SUPPLEMENTARY NOTATION

17. COSATI CODES			18. SUBJECT TERMS (Continue on reverse if necessary and identify by block number)
FIELD	GROUP	SUB-GROUP	
09	01		Antenna, Balun, Microstrip
20	14		

19. ABSTRACT (Continue on reverse if necessary and identify by block number)

A printed circuit dipole with integrated balun is presented that has achieved measured bandwidths of 40 percent over a 2:1 VSWR range. The microstrip balun features a double-tuning capability that provides the dipole with an impedance match over a wide band of frequencies.

Simple transmission line theory is used to analyze the balun structure, whereas the method-of-moments is utilized to determine the dipole current distribution. Two dipoles were fabricated and tested in order to validate the dipole/balun design equations. Antenna patterns are taken at several frequencies over the operating band to determine any frequency dependence of the patterns. VSWR measurements and cross-polarization patterns are also presented.

20. DISTRIBUTION/AVAILABILITY OF ABSTRACT ☐ UNCLASSIFIED/UNLIMITED ☒ SAME AS RPT ☐ DTIC USERS	21. ABSTRACT SECURITY CLASSIFICATION Unclassified
22a. NAME OF RESPONSIBLE INDIVIDUAL Paul M. Proudfoot, 2Lt, USAF	22b. TELEPHONE (Include Area Code) (617) 377-4036 22c. OFFICE SYMBOL RADC/EEAA

DD FORM 1473, 84 MAR — 83 APR edition may be used until exhausted. All other editions are obsolete.

SECURITY CLASSIFICATION OF THIS PAGE

Contents

Illustrations

A Wide-Band Printed Circuit Dipole

1. INTRODUCTION

This report documents the design and testing of a printed circuit dipole/balun configuration that has achieved measured bandwidths of 40 percent, over a 2:1 VSWR range.

General guidelines for the design of the dipole/balun was reported by Edward and Rees.[1] This report differs in that specific design equations are presented that will enable the design and fabrication of this element in-house. Additionally, antenna patterns were taken at the upper and lower end of the operating band to determine any frequency dependence of the patterns. Finally, cross-polarization patterns are presented.

Simple transmission line theory is used to analyze the balun structure, whereas, the method-of-moments is utilized to determine the dipole's input impedance.

The dipole/balun structure combines the moderate bandwidth of the dipole, with the double-tuning capability of the balun, to produce an element that has significantly greater bandwidth than conventional printed circuit patch radiators.

Because the dipole/balun configuration is a printed circuit element, it has the important advantages of being a low-cost and light-weight device.

Arrays of the future will frequently be made up of printed circuit elements in order to keep overall cost down; the dipole/balun element should prove to be attractive, because it does not trade-off any features found in some existing arrays. For example, all feed lines and active devices are located behind the antenna element. Here they won't interfere with tight interelement spacings. Also, a metal

---

(Received for Publication 13 May 1988)

1. Edward, B. and Rees, D. (1987) A broadband printed dipole with integrated balun, *Microwave J.* **30**: 339-344.

ground plane shields the antenna half-space from spurious radiation emitted by feed lines and active devices. This will prevent degradation of sidelobe levels, polarization, and gain in an array environment.

2. MODEL

2.1 The Balun

The key to the wide-band operation of the dipole/balun configuration is the double-tuning capability of the balun. The wide-band balun used in this experiment was first proposed by Roberts[2], was later put into printed circuit form by Bawer and Wolfe[3] and was most recently used by Edward and Rees[1] in a similar experiment. Figure 1 illustrates the geometry of the printed circuit dipole/ balun. The coaxial equivalent[3] to the printed circuit is shown in Figure 2.

In the coaxial circuit, the dipole input impedance is simply represented by a complex value (Z_d). By inspection of the circuit of Figure 2, the input impedance (Z_{in}) can be expressed as:

$$Z_{in} = -j\, Z_a \cot \theta_a + \frac{j\, Z_d\, Z_{ab} \tan \theta_{ab}}{Z_d + j\, Z_{ab} \tan \theta_{ab}} \tag{1}$$

where Z_a, θ_a, Z_{ab}, and θ_{ab} are the characteristic impedance and electrical length, of the microstrip and coupled microstrip lines respectively. By judicious selection of the parameters θ_a and θ_{ab} (that is, the open-end length and slot length) in Eq. 1, one can achieve an impedance match over a very wide bandwidth. The rest of this section is devoted to determining the balun parameters Z_a, θ_a, Z_{ab}, and θ_{ab}.

The characteristic impedance (Z_a) of a microstrip line of width (W), on a substrate thickness (h), dielectric constant (ε_r), and foil thickness (t) is [4:62],

$$Z_a = \begin{cases} \dfrac{\eta}{2\pi\sqrt{\varepsilon_{eff}}} \ln\left[\dfrac{8h}{W_e} + .025\,\dfrac{W_e}{h}\right] & \dfrac{W}{h} \le 1 \\[2ex] \dfrac{\eta}{\sqrt{\varepsilon_{eff}}}\left[\dfrac{W_e}{h} + 1.393 + .667 \ln\left(\dfrac{W_e}{h} + 1.444\right)\right]^{-1} & \dfrac{W}{h} \ge 1 \end{cases} \tag{2}$$

where η is the impedance of free space, $120\,\pi$. W_e is the effective line width, which accounts for fringing fields near the strip edge:

$$W_e = W + 1.25t\delta/\pi$$

$$\delta = \begin{cases} 1 + \ln(4\pi\, W/t) & \dfrac{W}{h} \le \dfrac{1}{2\pi} \\[2ex] 1 + \ln(2h/t) & \dfrac{W}{h} \ge \dfrac{1}{2\pi} \end{cases} \tag{3}$$

---

2. Roberts, W.K. (1957) A new wide-band balun, *Proc. IRE* **45**: 1628-1631.
3. Bawer, R. and Wolfe, J.J. (1960) A printed circuit balun for use with spiral antennas, *IRE Trans. on Microwave Theory Tech.* **MTT-8**:319-325.
4. Gupta, K.C., Garg, R., and Chadha, R. (1981) *Computer Aided Design of Microwave Circuits*, Artech House, Dedham, MA.

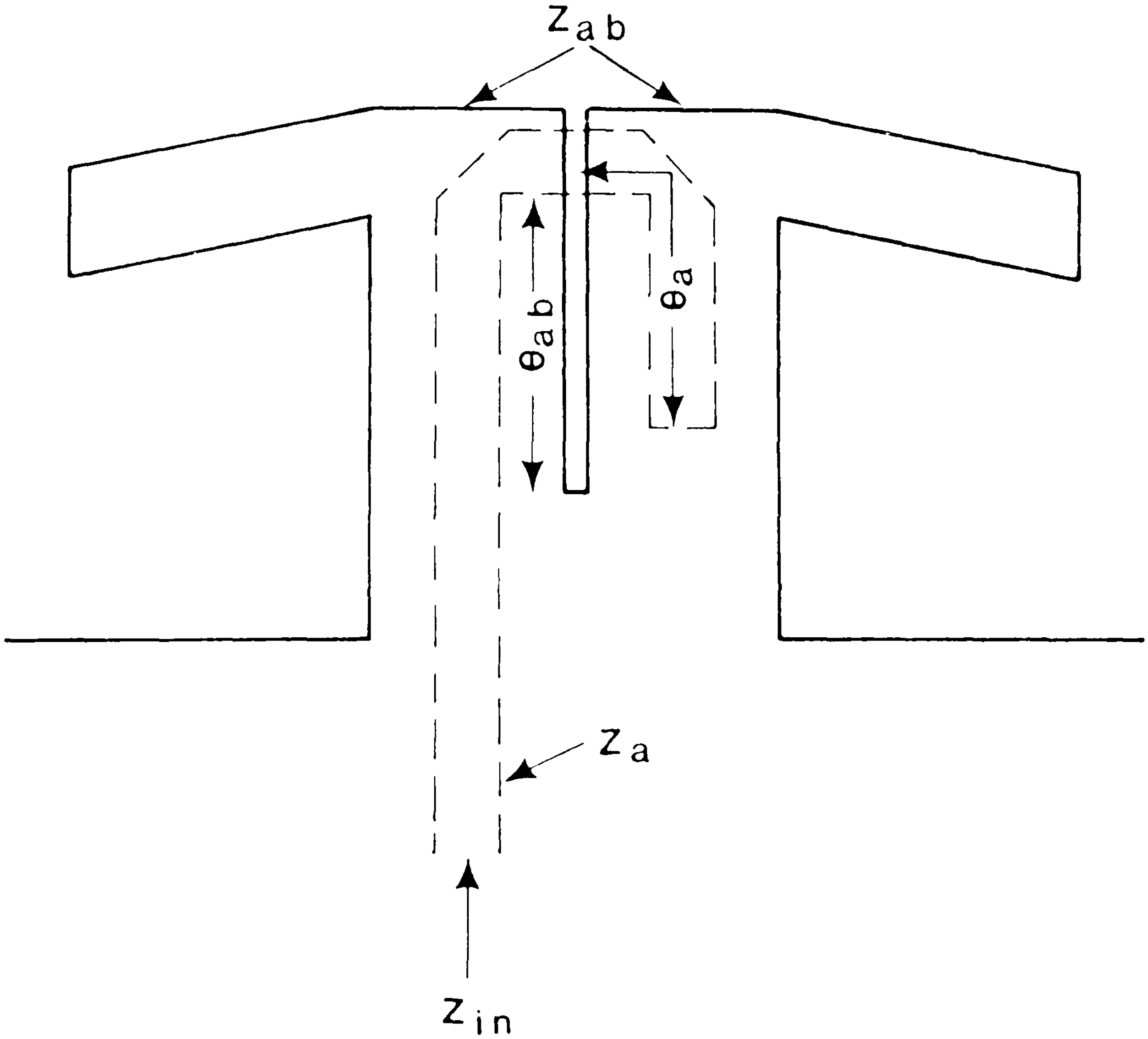

Figure 1. Dipole/Balun Geometry

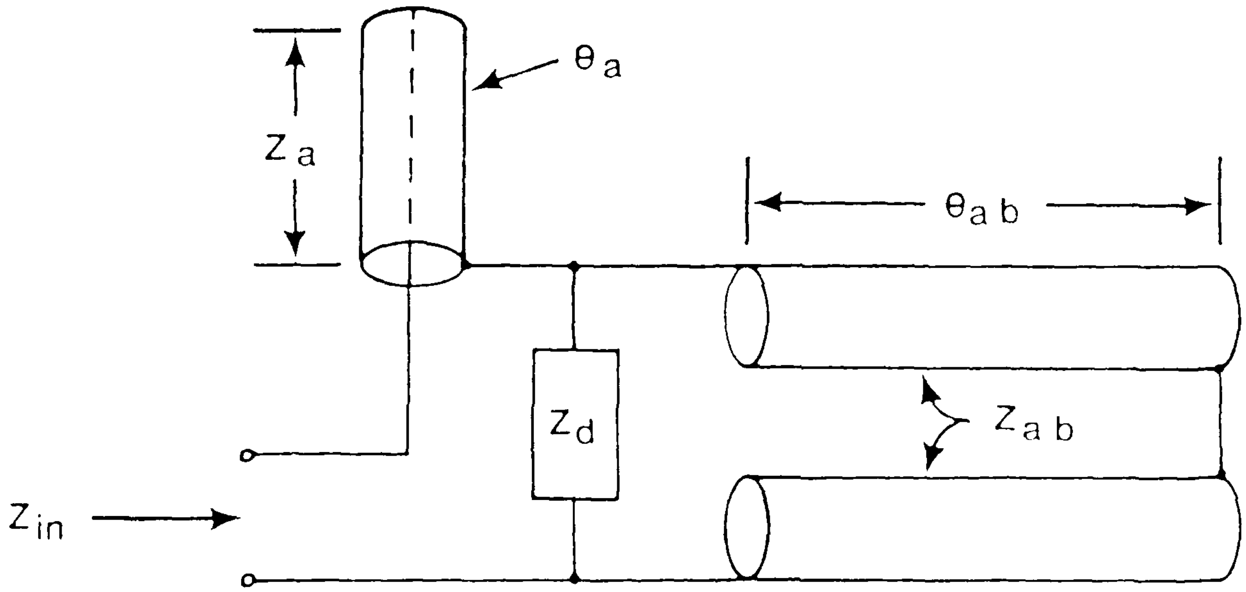

Figure 2. Coaxial Equivalent Circuit

A FORTRAN subroutine that calculates the correct microstrip width for a given impedance and substrate, can be found in RADC-TM-86-08[5].

When calculating the electrical length θ_a and characteristic impedance Z_a of the microstrip line, the effective dielectric constant

$$\varepsilon_{eff} = \frac{\varepsilon_r + 1}{2} + \frac{\varepsilon_r - 1}{2}\left[1 + \frac{10h}{W}\right]^{-1/2} - \frac{\varepsilon_r - 1}{4.6}\,\frac{t/h}{\sqrt{W/h}} \qquad (4)$$

is used.

The electrical length θa is then:

$$\theta_a = \frac{2\pi}{\lambda_\varepsilon} l_a$$

where

$$\lambda_\varepsilon = \frac{\lambda_o}{\sqrt{\varepsilon_{eff}}} \qquad (5)$$

and λ_o is the free space wavelength. The physical length l_a of the microstrip line is measured beginning at the mid-point between the two coupled microstrip lines (see Figure 1), runs along the inside edge of the mitered bend, and terminates at the open end. The length extension [4:190]

$$\Delta l = .412h\,\frac{(\varepsilon_{eff} + .3)}{(\varepsilon_{eff} - .258)}\quad\frac{(W/h + .264)}{(W/h + .8)} \qquad (6)$$

is then added to l_a to account for fringing fields that occur at the open-end discontinuity.

Values for Z_{ab} and θ_{ab} are determined using the odd-mode characteristic impedance and effective dielectric constant of a coupled microstrip line. There are several good references in which these equations can be found[4,6]. One reference in particular[7] gave closed form, easy-to-use equations that are accurate even into the millimeter-wave region. The physical length used in determining θ_{ab} is measured from the lower edge of the microstrip line (see Figure 1) to the bottom of the slot.

Selecting a suitable substrate is a critical step in the design of a dipole with integrated balun. Once a substrate is selected, the designer has very little freedom to vary microstrip and coupled microstrip line widths. In the balun structure, the coupled microstrip line essentially acts as ground plane to the microstrip line (see Figure 3). Note in this figure, that virtually all of the fields beneath the microstrip line of width W are contained within 3W[2]. Therefore, the width of the coupled microstrip line must be greater than 3W. Since there are 2 coupled microstrip lines, the dimension B (in Figure 3) must be greater than 6W. This transverse dimension B is now a major limitation to both

---

5. McGrath, D.T., Mullinix, D.A., and Huck, K.D. (1986) *FORTRAN Subroutines for Design of Printed Circuit Antennas*, RADC-TM-86-08, ADB107263L.
6. Akhtarzad, S., Rowbotham, T.R., and Johns, P.B. (1975) The design of coupled microstrip lines, *IEEE Trans. Microwave Theory Tech.* **MTT-23:**486-492.
7. Kirschning, M. and Jansen, R.H. (1984) Accurate wide-range design equations for the frequency-dependent characteristics of parallel coupled microstrip lines, *IEEE Trans. Microwave Theory Tech.* **MTT-32**:83-90.

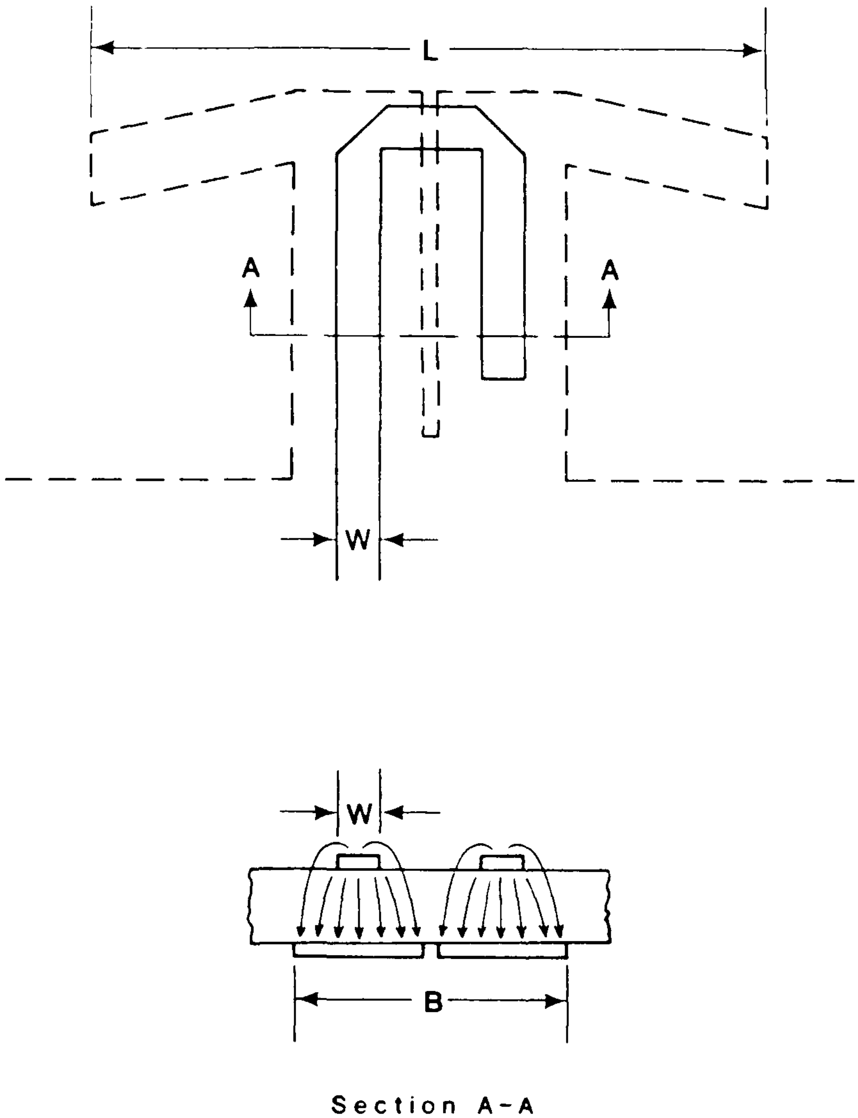

Figure 3. Fields Beneath a Microstrip Line

the upper value of Z_{ab} and to the maximum frequency for which a dipole can be fabricated on a particular substrate. For example, the dipole length (L) is approximately 0.43λ, or 0.42 in. at 12 GHz. Obviously, this dipole could not be put on a substrate that yields a dimension B equal to 0.6 inches, because the 2 coupled microstrip lines would be wider than the dipole. To keep all dipole/balun dimensions in proportion, it is suggested that $.4L < B < .5L$. Finally, a substrate should be selected so that the substrate appears electrically thin ($h/\lambda_\varepsilon < .1$). This constraint will help insure that the equations used in determining Z_a, θ_a, Z_{ab}, and θ_{ab} will yield accurate results.

2.2 The Dipole

The last parameter to be determined is the dipole's input impedance (Z_d). Here, a flat radiating dipole, of arm width D, is modeled as a thin wire antenna with a diameter equal to D/2[8]. The method-of-moments is then applied to Hallen's integral equation to determine the current distribution, and hence the input impedance of the dipole. Balanis[9] contains a computer program, written in FORTRAN, that uses the method-of-moments to determine the current distribution, input impedance, and radiation pattern of a finite diameter dipole. Figure 4 shows a typical printed dipole input impedance as calculated with this program.

3. RESULTS

3.1 Dipole Fabrication

In order to demonstrate the broadband operation of the dipole/balun configuration, two dipoles were fabricated on 1/16 in. thick substrate, commercial designation OAK-602®, with dielectric constant 2.54. Figure 5 shows one of the dipoles mounted $\lambda_0/4$ above a 16 x 16 in. ground plane. Both dipoles have an arm width of 0.16 in. and have a total arm length (L) of 1.20 in. and 1.34 in., respectively. A length extension, equal to 1/4 of a dipole arm width, was added to L in order to account for radiation effects from the ends of the dipole.

Both dipoles have an input impedance of about 75Ω at resonance, therefore, a 75Ω microstrip line is used to feed them. A 61Ω quarter-wave transformer is then utilized to match the microstrip line to a 50Ω jack-tab connector.

3.2 VSWR Measurements

Figure 6 shows the measured and theoretical results of the two dipoles that were fabricated. SWR measurements were made on a HP8408A Automatic Network Analyzer with the dipoles mounted $\lambda_0/4$ above the ground plane. Note in Figure 6a and 6b that neither dipole is optimized for maximum

---

8. Butler, C.M. (1982) The equivalent radius of a narrow conducting strip, *IEEE Trans. Antennas Propag.* **AP-30**:755-758.
9. Balanis, C.A. (1982) *Antenna Theory*, Harper and Row, New York, pp. 319-321.

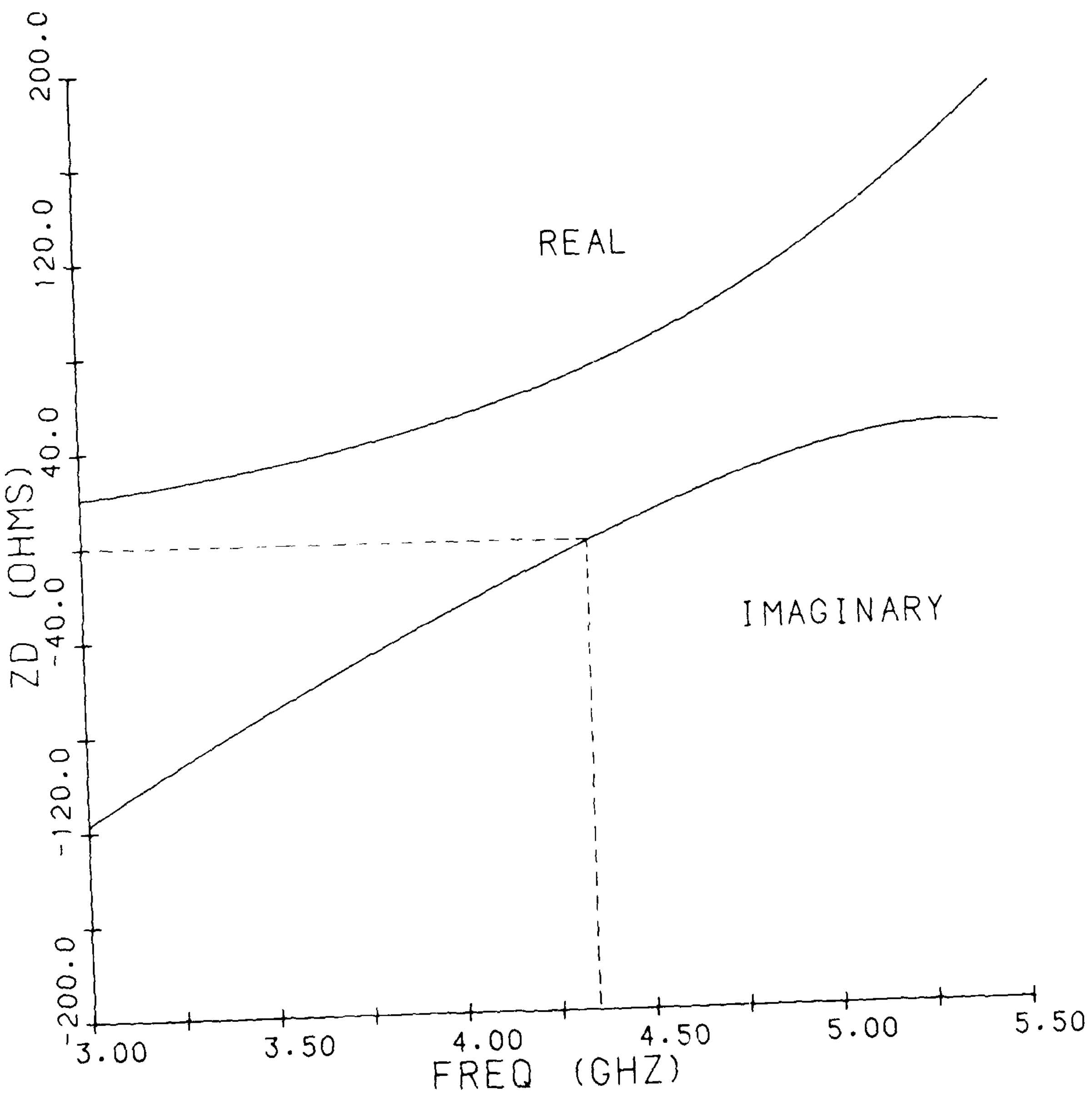

Figure 4. Input Impedance of a Dipole

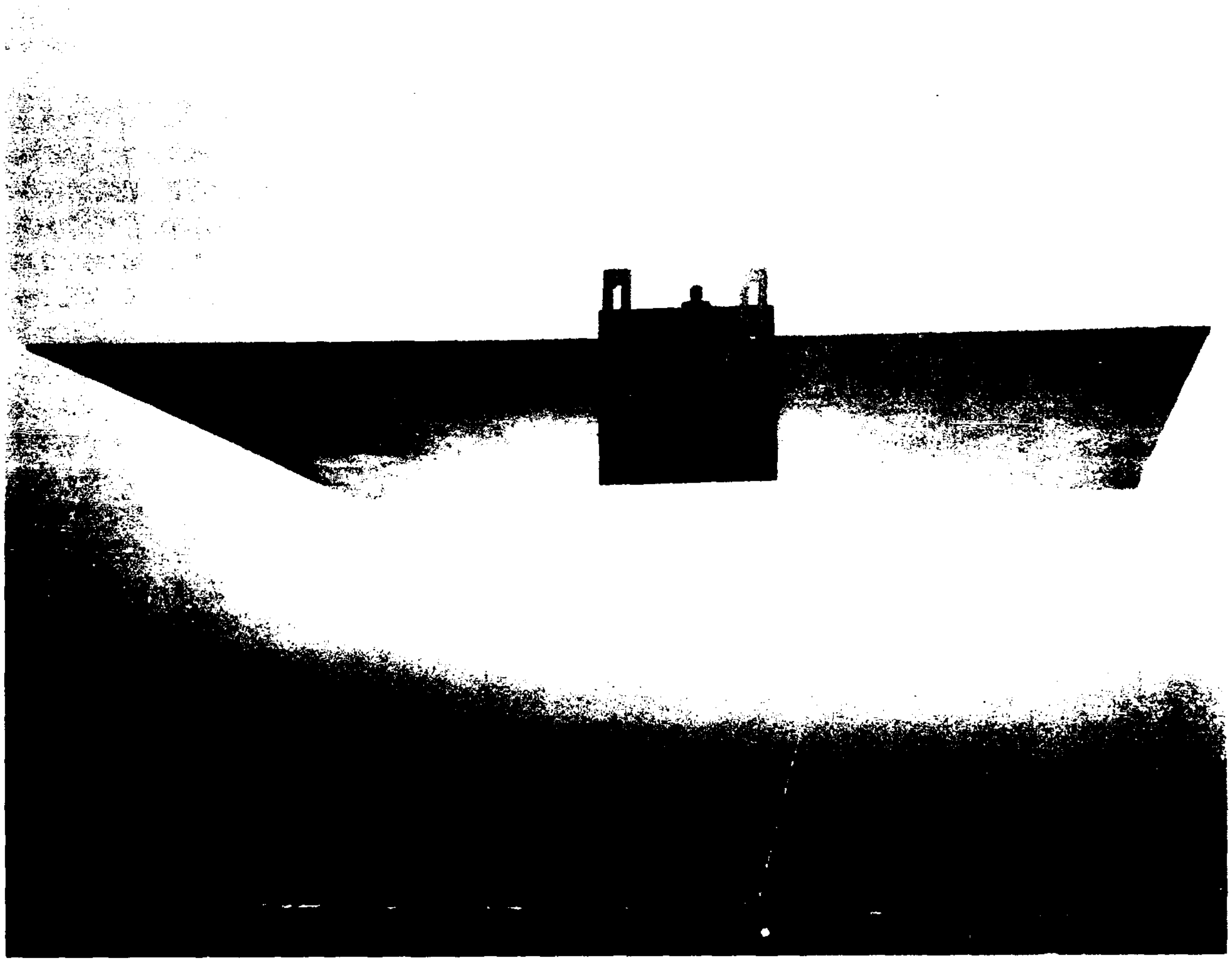

Figure 5. Printed Circuit Dipole Mounted above a Ground Plane

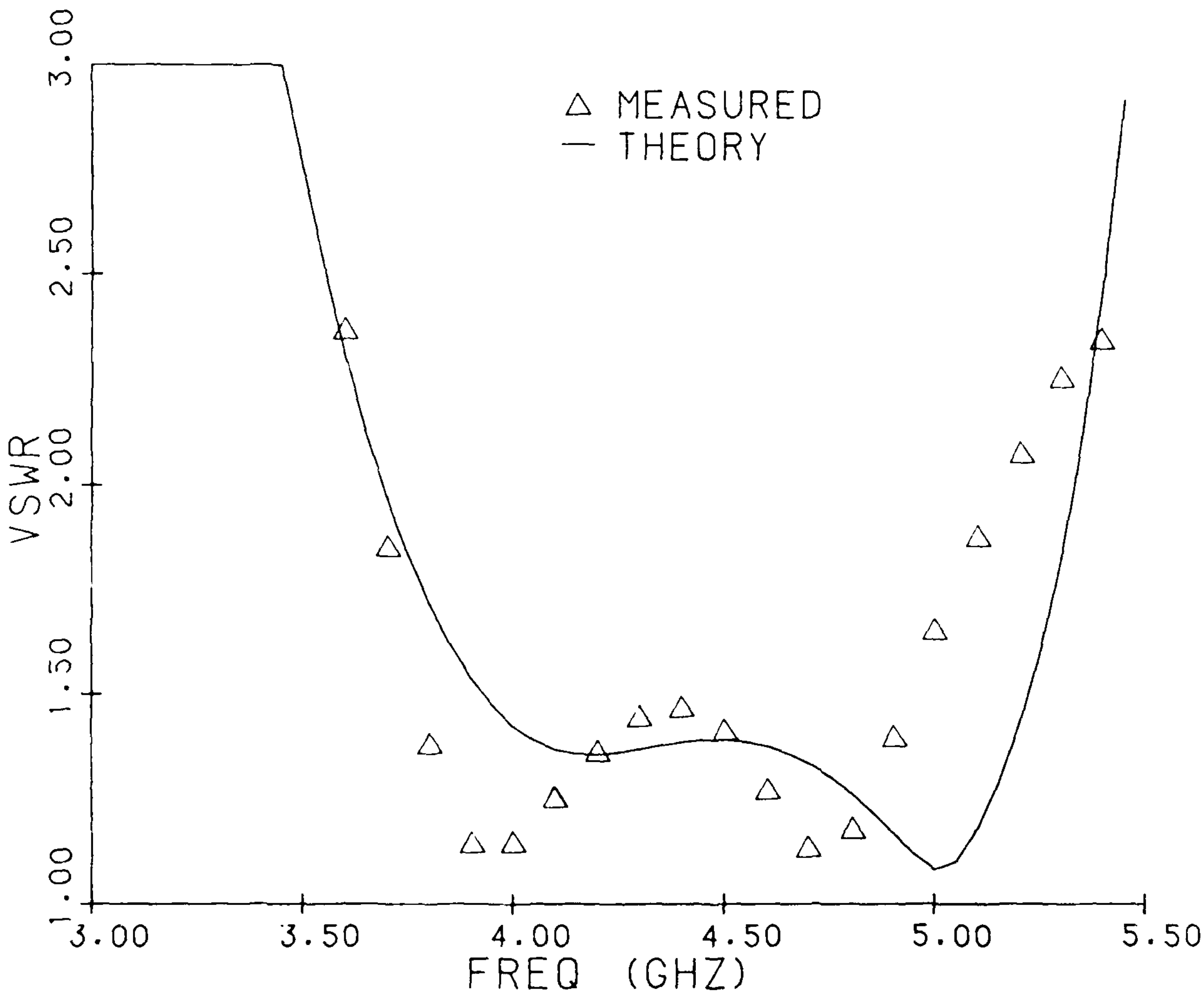

Figure 6a. Measured and Theoretical VSWR. 1.2 in. Dipole

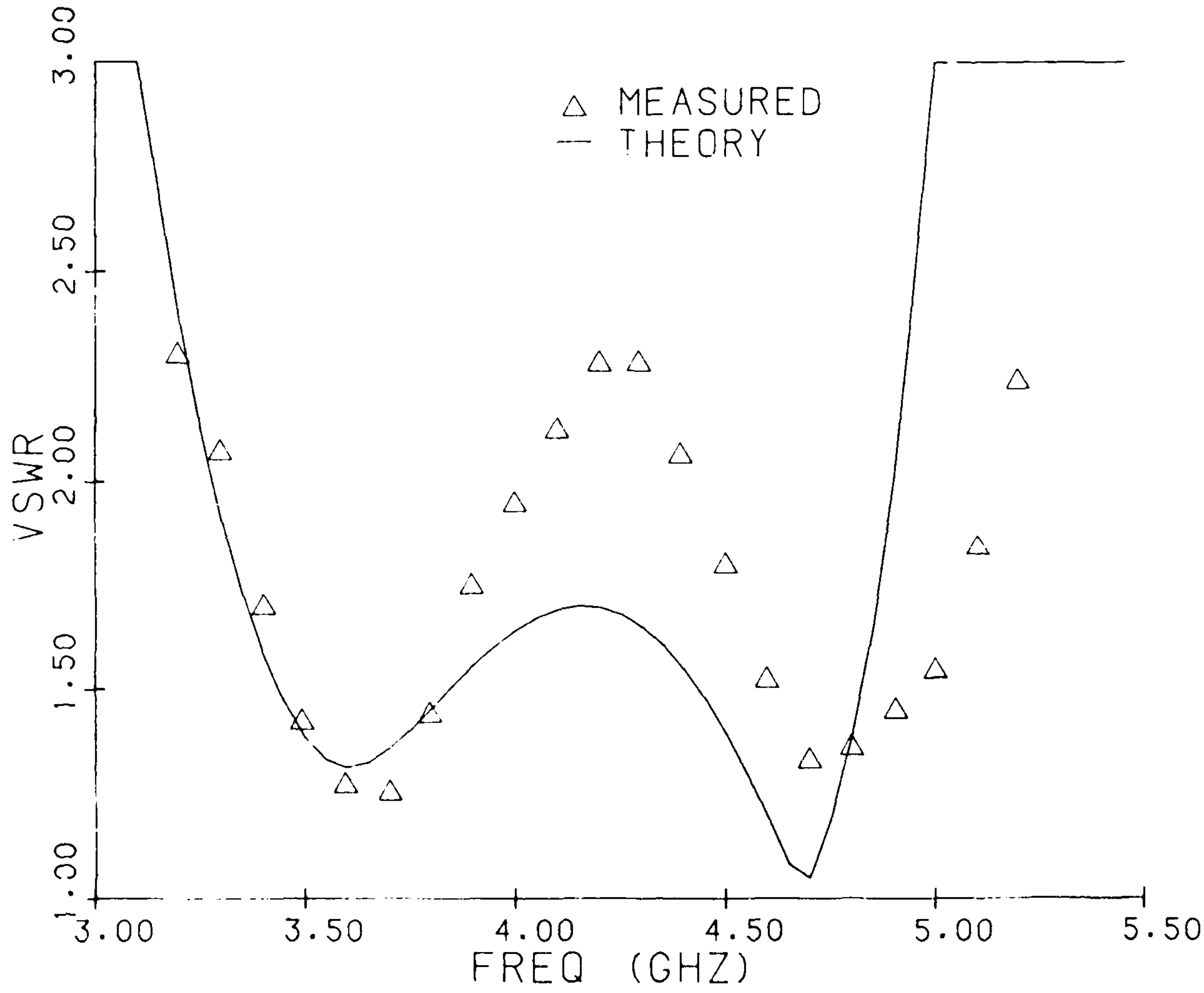

Figure 6b. Measured and Theoretical VSWR: 1.34 in. Dipole

bandwidth, according to the SWR < 2 criterion. The measured SWR goes slightly above 2 in Figure 6b for a "potential" bandwidth of 43.5 percent, and the SWR is well below 2 in Figure 6a for a bandwidth of 33.3 percent.

A dipole can be optimized for maximum bandwidth by trimming the slot length of the coupled microstrip line and/or the open-end length of the microstrip line. When the balun is trimmed in this manner, the effect is to move the second resonance in Figure 6 up or down in frequency, as the first resonance stays relatively constant. Another effect of trimming is that the dipole's resonance appears slightly below center band. For example, in Figure 4 the 1.2 in. dipole resonates at about 4.38 GHz. Note the theoretical curve in Figure 6a, in which 4.38 GHz appears slightly below center band. This is characteristic of the dipole/balun configuration. It is suggested that the slot length be etched slightly shorter, and the open-end slightly longer than expected. It is much easier to remove copper from, than add copper to, a substrate.

3.3 Antenna Patterns

Measured E– and H– plane patterns of the two dipoles are shown in Figures 7 and 8. It was noted while taking pattern measurements that there should be good electrical contact between the aluminum ground plane and the substrate's ground plane. Patterns will be moderately degraded if this precaution is not adhered to. Also, a metal housing was used to enclose hardware located behind the aluminum ground plane. This eliminated any contributions to the antenna pattern from spurious radiation emitted by the feed line and the coax-to-microstrip transition.

Next, patterns were taken of the 1.2 in. dipole at the upper and lower end of the operating band to determine any frequency dependence of the patterns. The results are shown in Figures 9 and 10. Comparing Figure 9a to Figure 10a, it can be seen that the E–plane patterns became slightly broader as frequency is increased from 3.6 to 5.0 GHz, especially when the antenna was rotated more than 40° from broadside. The only explanation for this seems to be that radiation from the dipole/balun configuration is more complicated than just that of the dipole itself.

From the few patterns that were taken, it was felt that radiation from the open-ended microstrip line accounts for a good portion of the change in dipole pattern with frequency. Since the dipole/balun will eventually be put into an array, further study of the single element radiation pattern was not pursued.

Finally, cross-polarization patterns are shown in Figure 11. Because of possible reflections in the anechoic chamber used in the measurement, patterns that go below –20 dB become questionable.

4. CONCLUSION

The broad-band operation of a printed circuit dipole with integrated balun was demonstrated. Measured bandwidths of 40 percent were obtained. Measured and theoretical results show good agreement. Antenna patterns show slight frequency dependence. Simple, easy-to-use, design equations were presented, that lend themselves nicely toward computer-aided design. This device should find many applications as a broad-band, low-cost and light-weight array element, that is capable of tight interelement spacings.

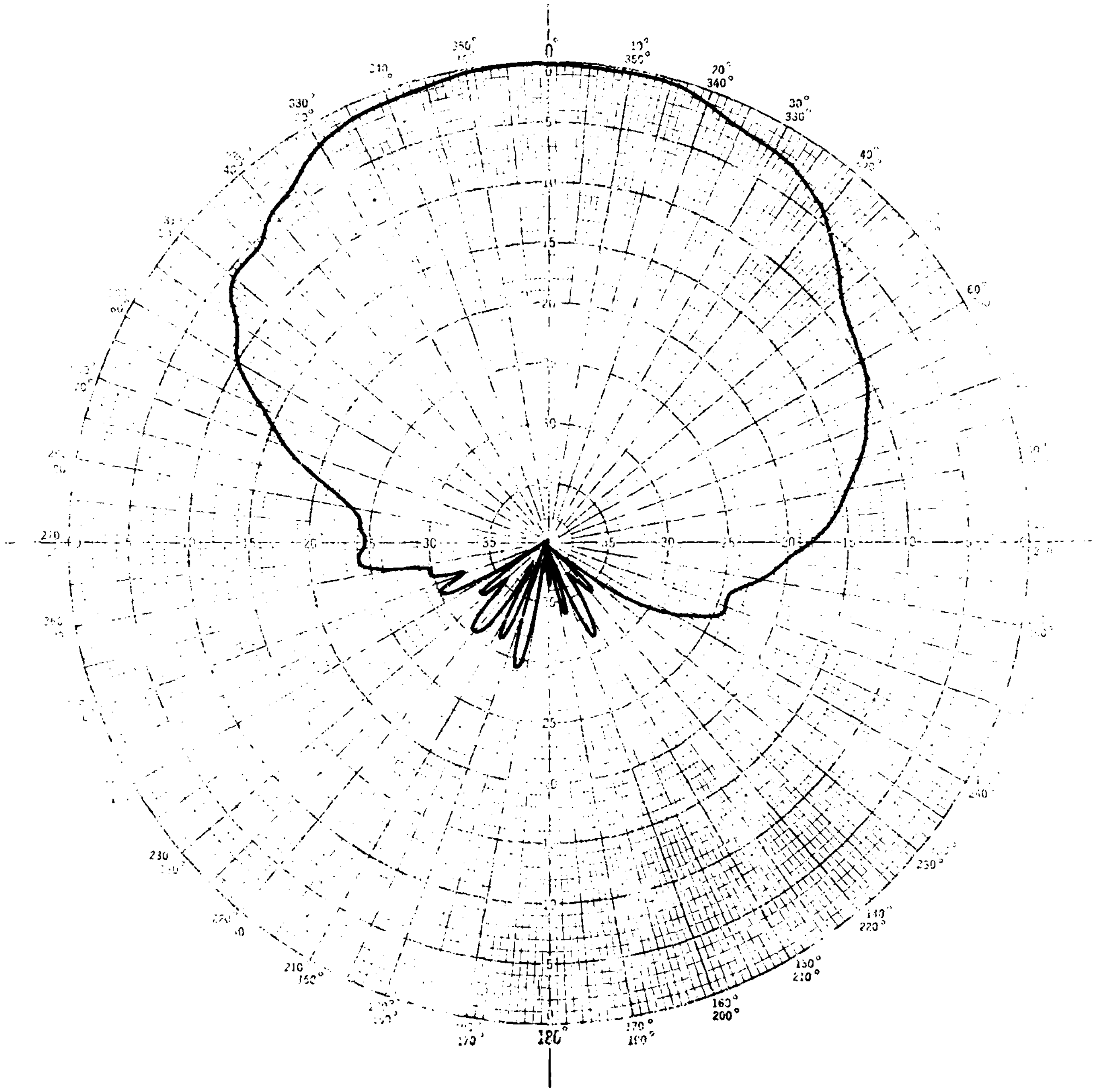

Figure 7a. Antenna Patterns 1.2 in. Dipole, 4.31 GHz: E-Plane

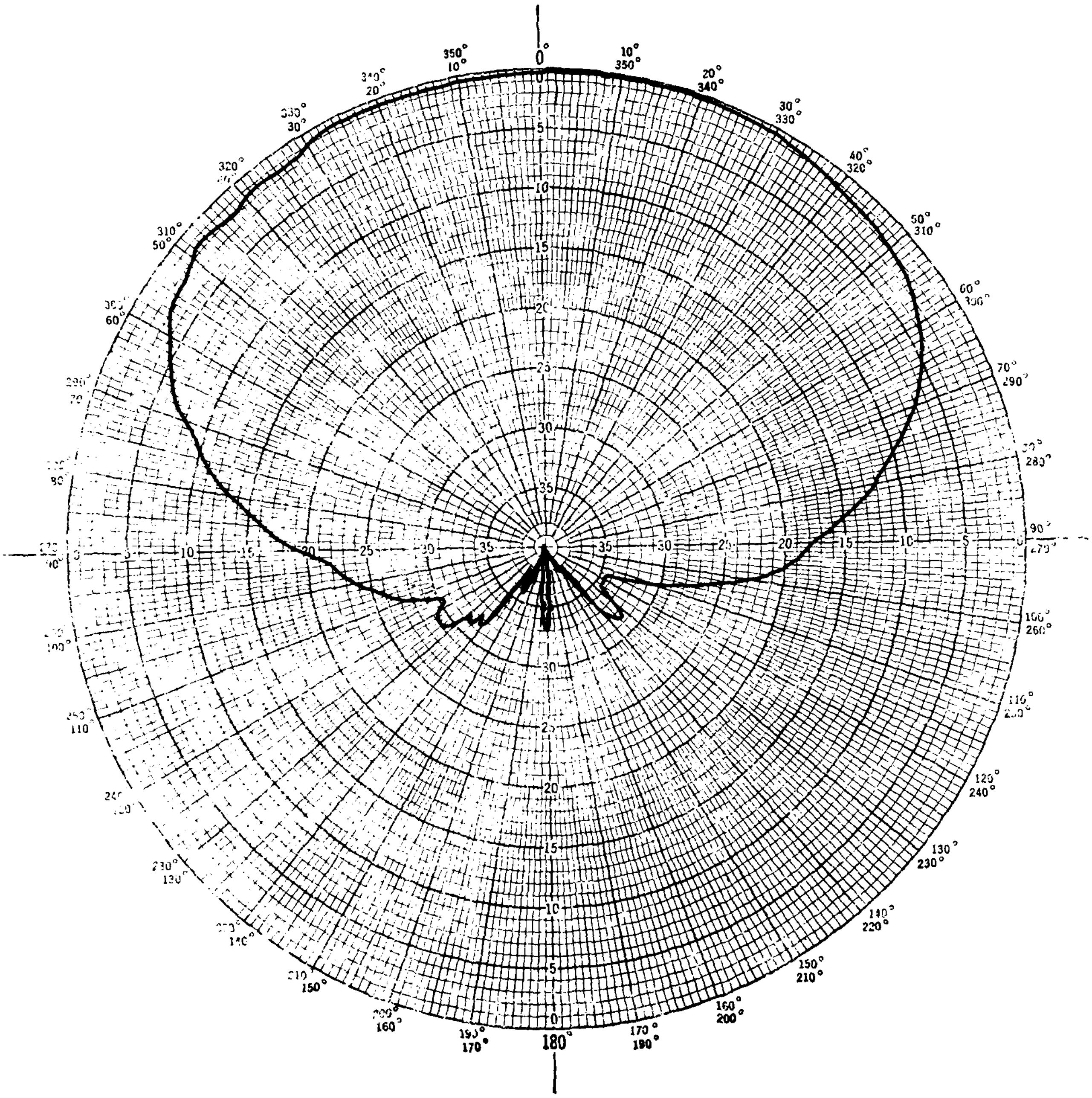

Figure 7b. Antenna Patterns 1.2 in. Dipole, 4.31 GHz: H-Plane

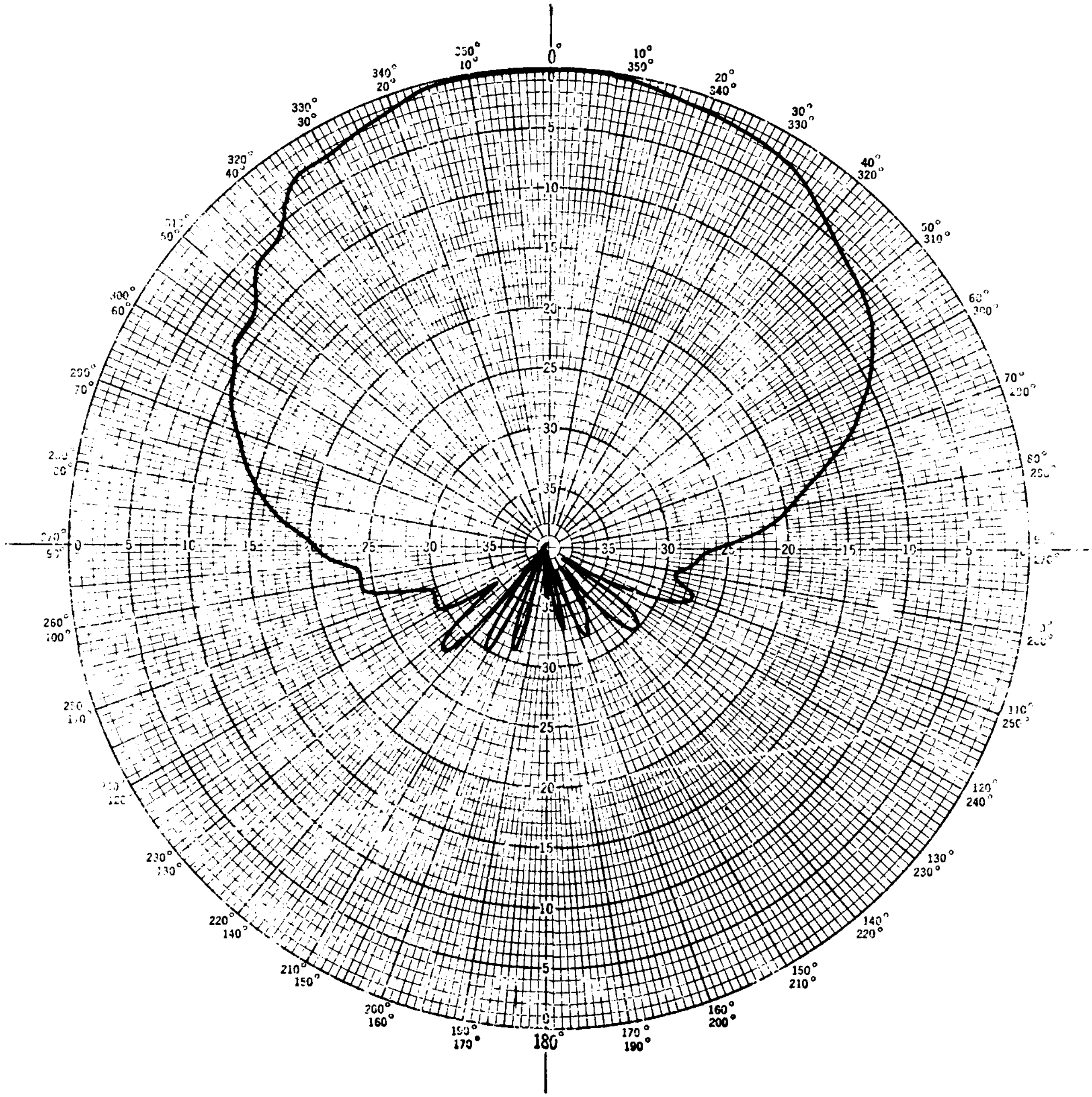

Figure 8a. Antenna Patterns 1.34 in. Dipole, 4.13 GHz: E-Plane

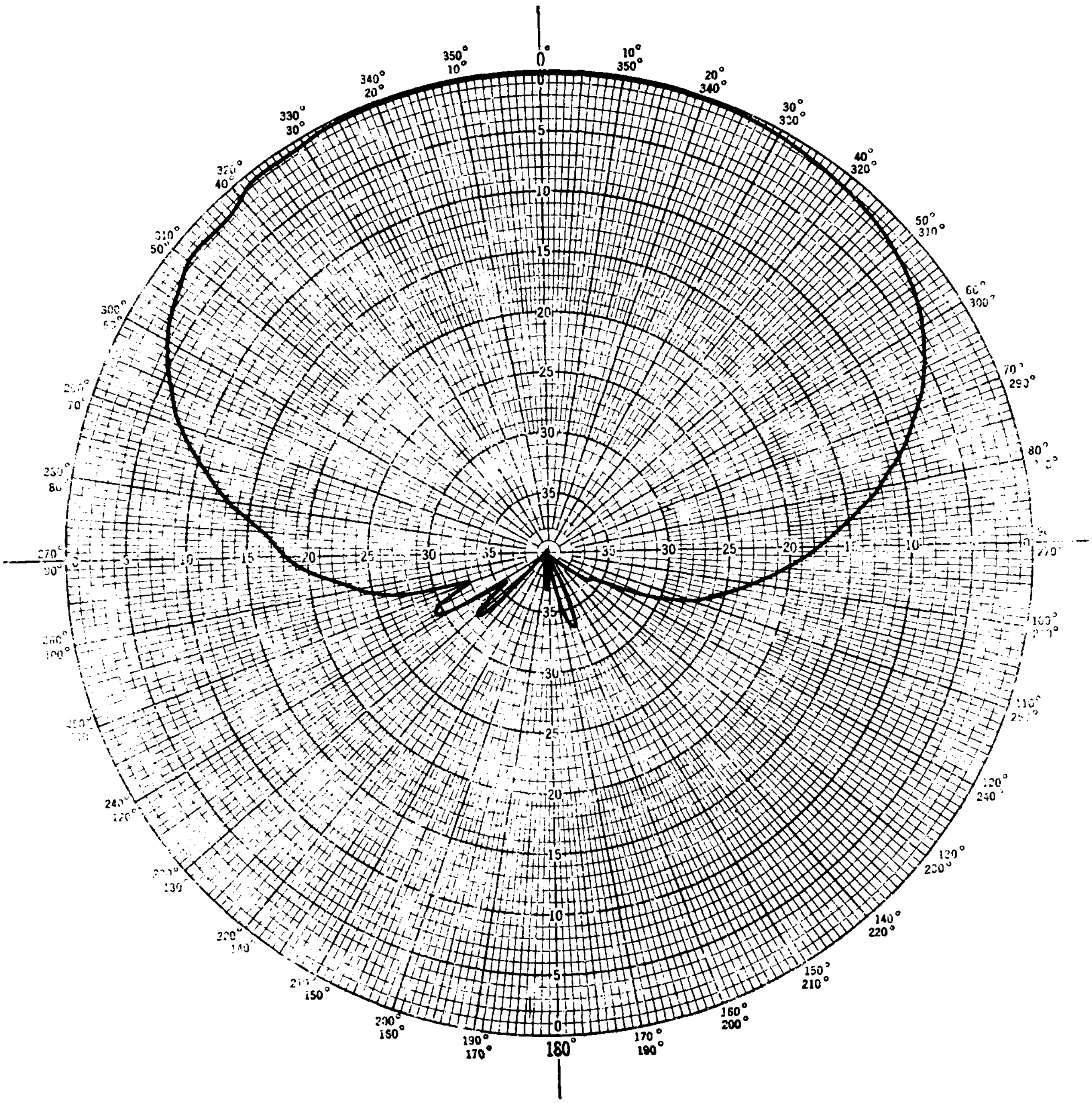

Figure 8b. Antenna Patterns 1.34 in. Dipole, 4.13 GHz: H-Plane

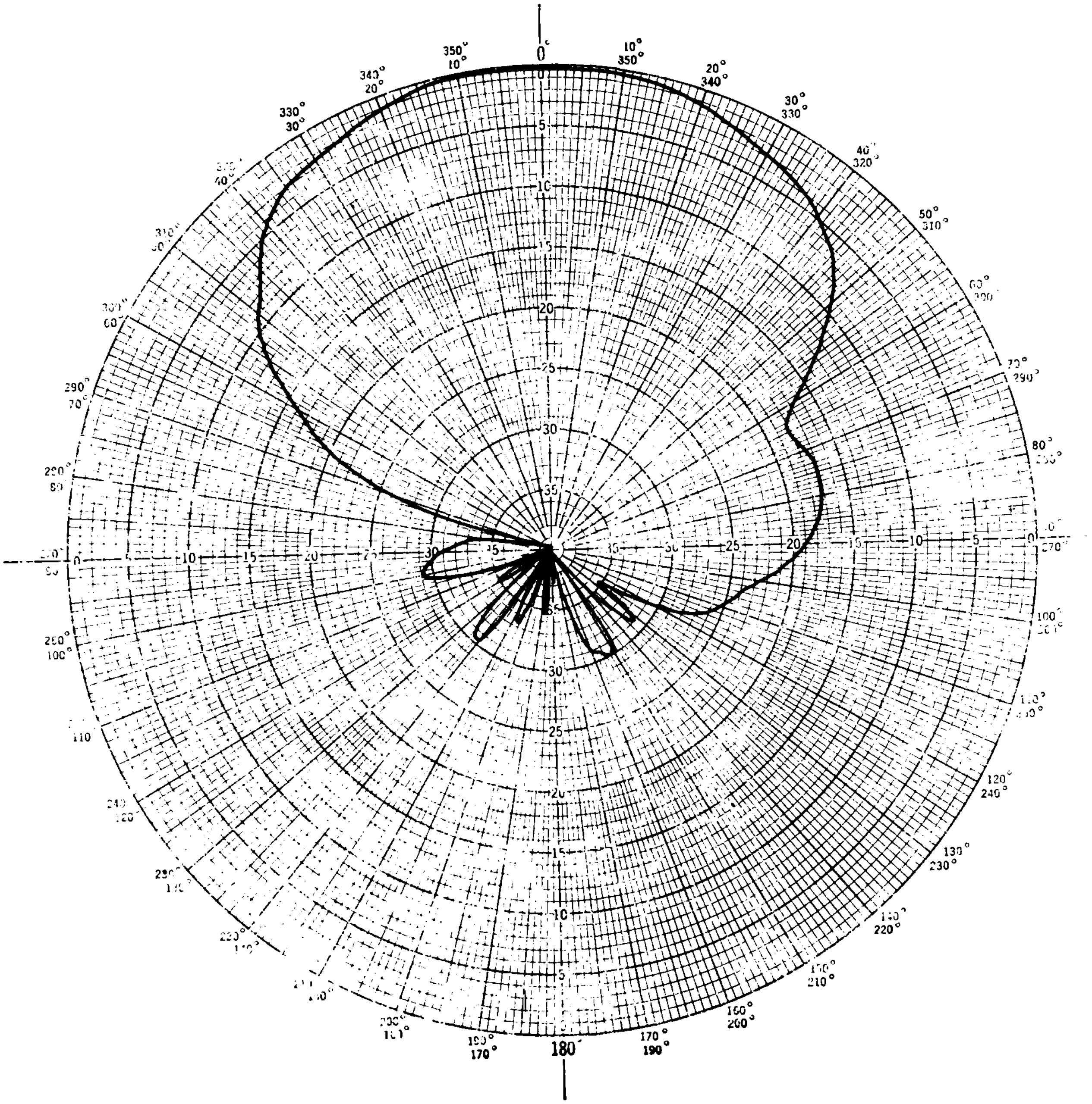

Figure 9a. Antenna Patterns 1.2 in. Dipole, 3.6 GHz: E-Plane

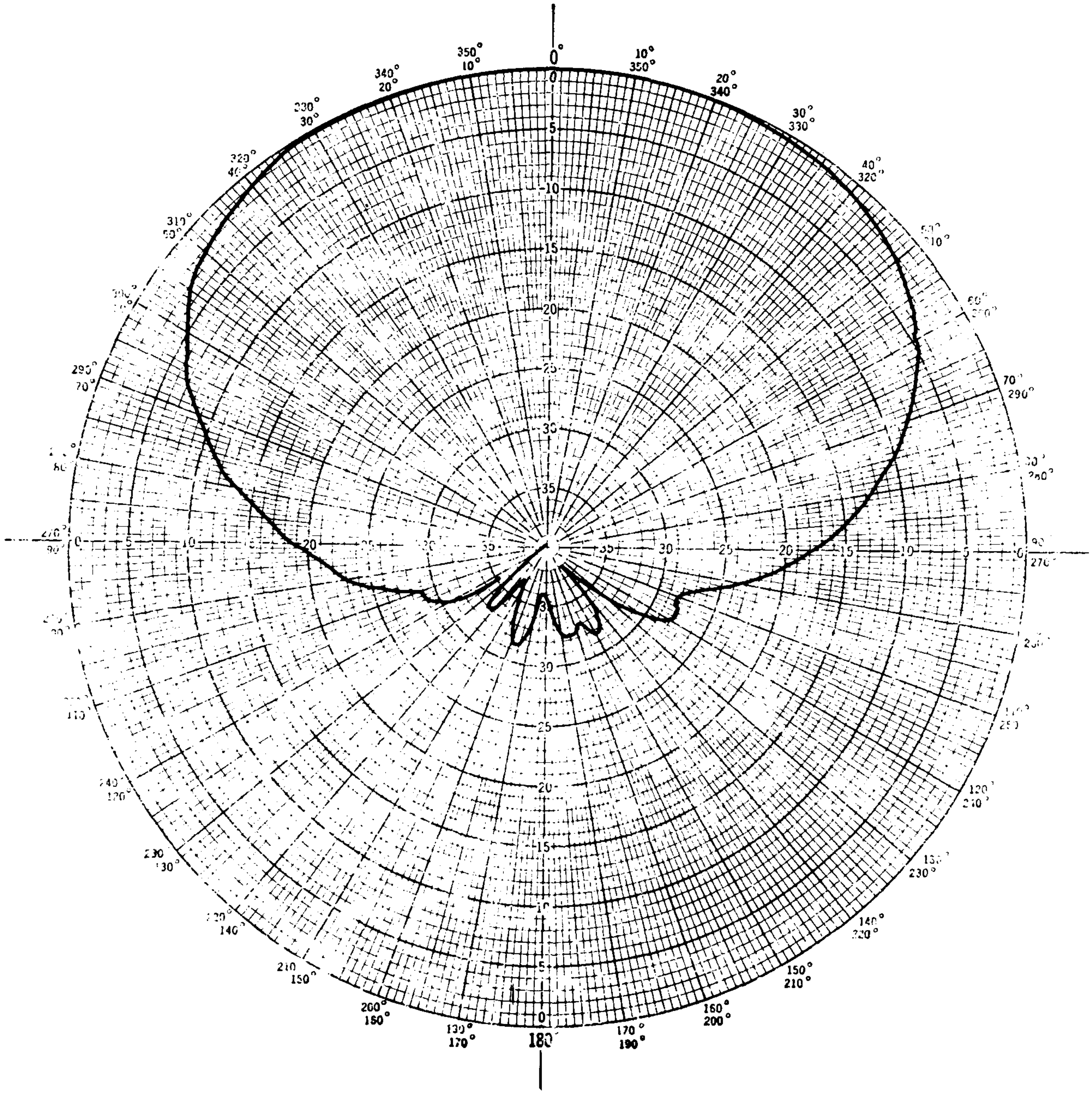

Figure 9b. Antenna Patterns 1.2 in. Dipole, 3.6 GHz: H-Plane

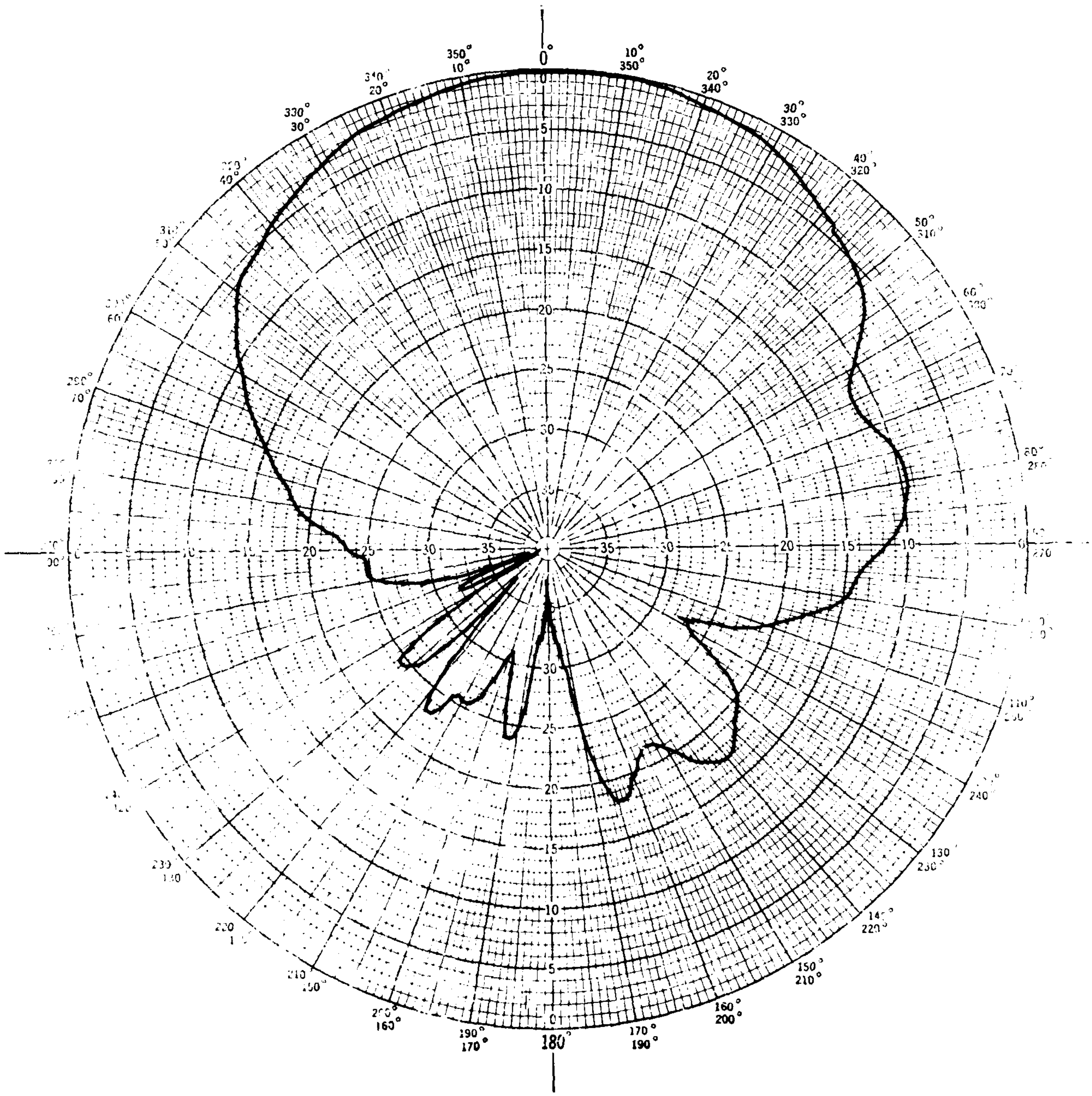

Figure 10a. Antenna Patterns 1.2 in. Dipole, 5.0 GHz: E-Plane

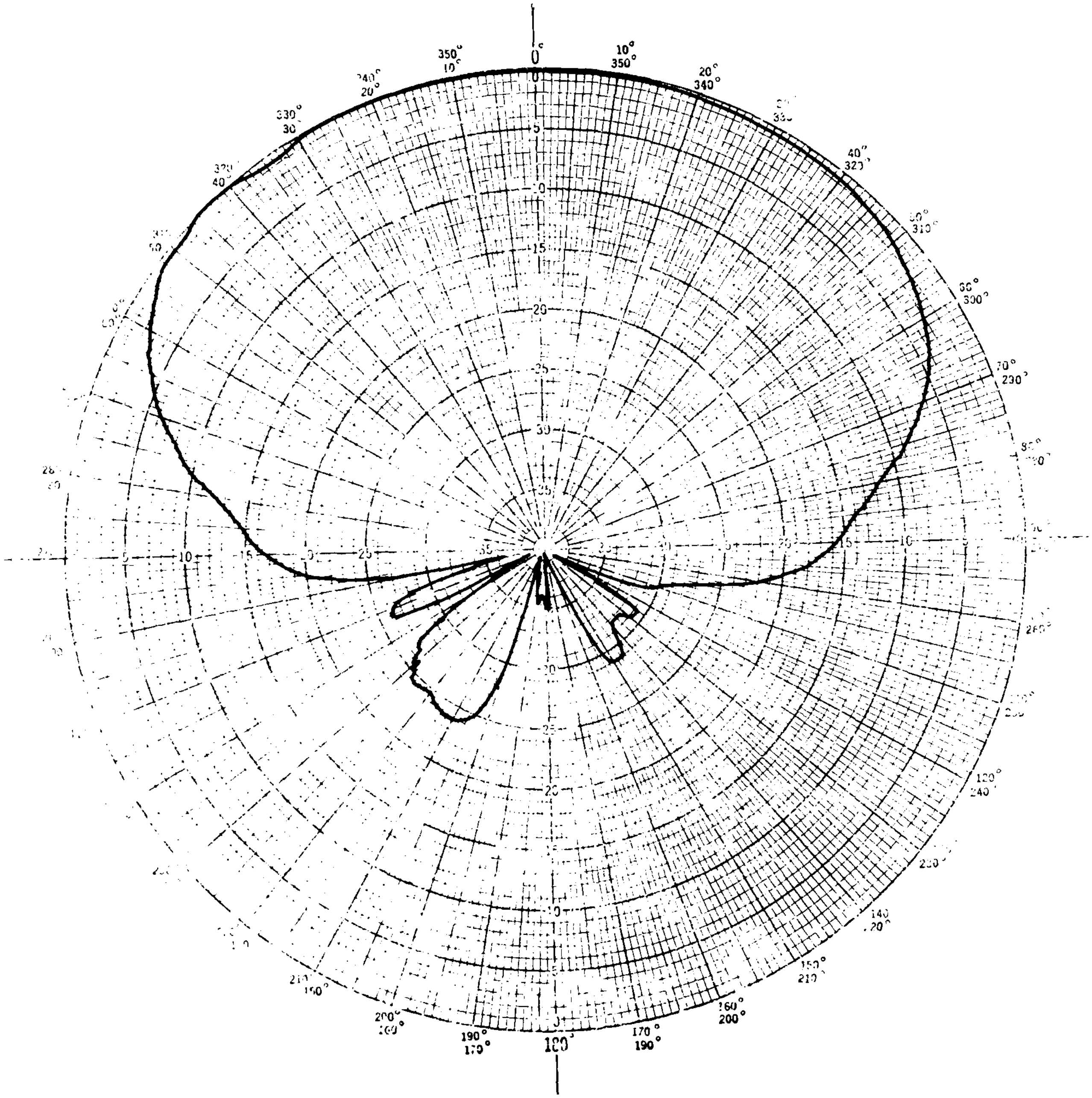

Figure 10b. Antenna Patterns 1.2 in. Dipole, 5.0 GHz: H-Plane

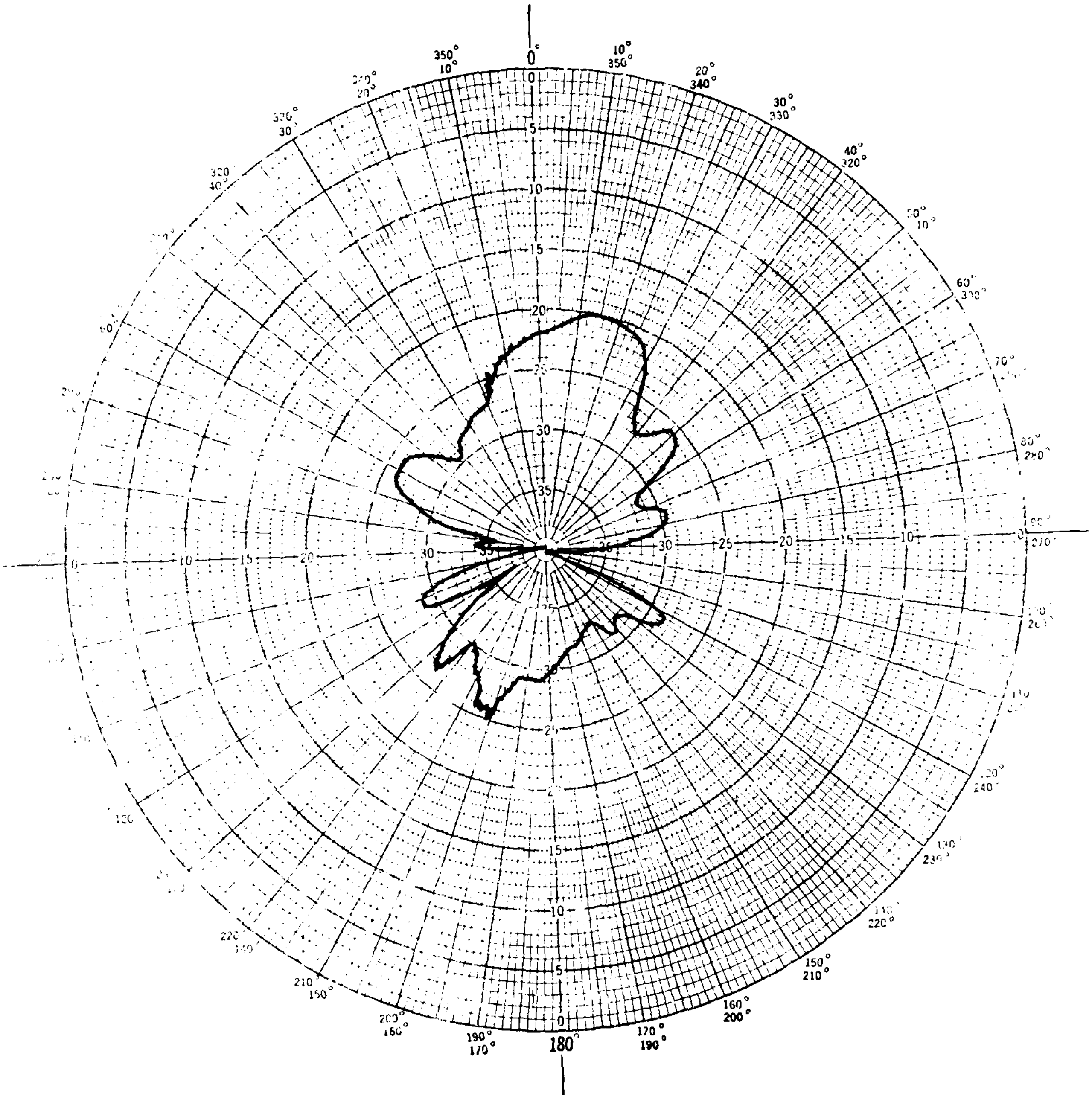

Figure 11a. Cross-Polarized Patterns 1.2 in. Dipole, 4.31 GHz: E-Plane

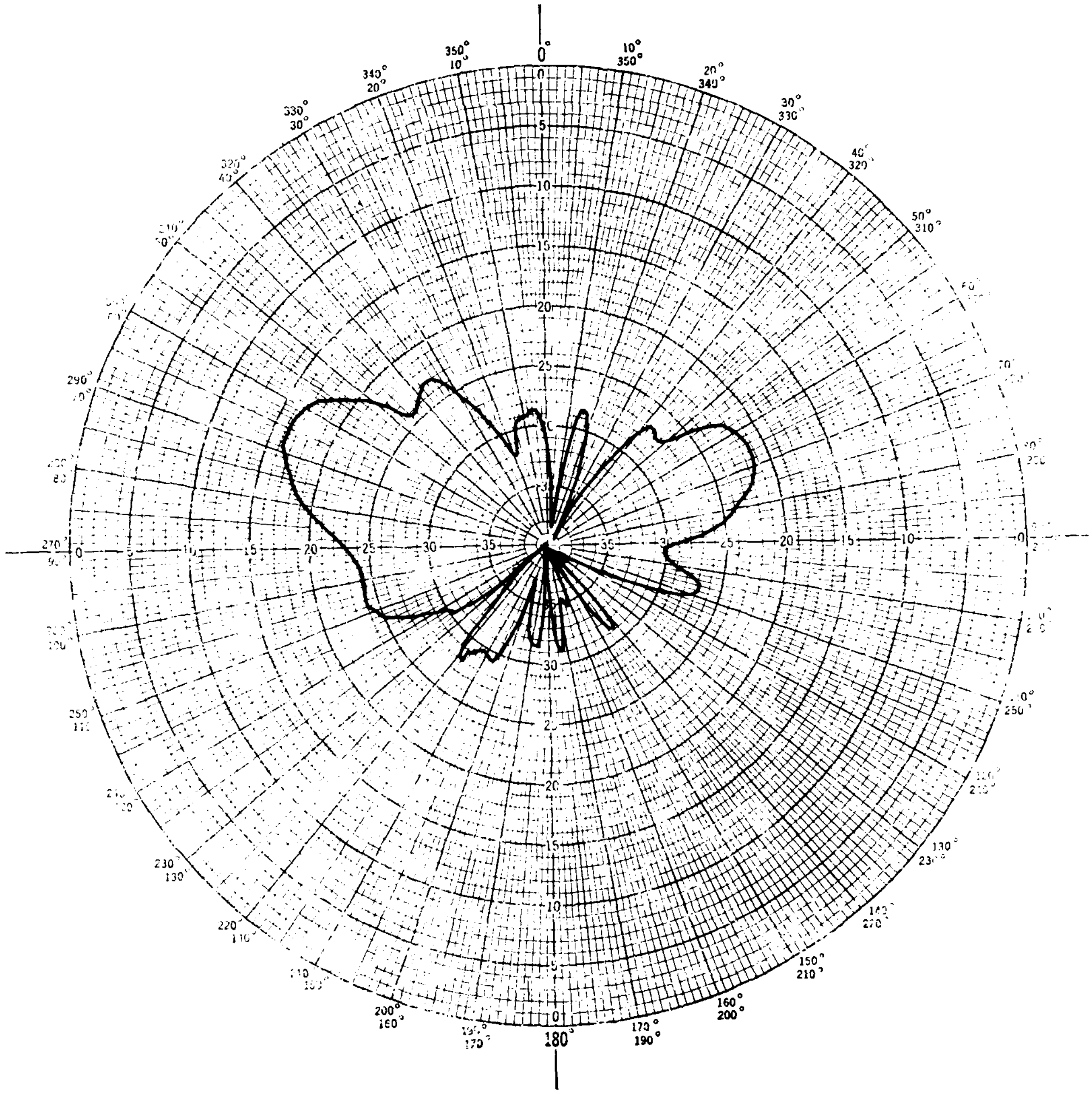

Figure 11b. Cross-Polarized Patterns 1.2 in. Dipole, 4.31 GHz: H-Plane

References

1. Edward, B. and Rees, D. (1987) A broadband printed dipole with integrated balun, *Microwave J.* **30**: 339-344.
2. Roberts, W.K. (1957) A new wide-band balun, *Proc. IRE* **45**: 1628-1631.
3. Bawer, R. and Wolfe, J.J. (1960) A printed circuit balun for use with spiral antennas, *IRE Trans. on Microwave Theory Tech.* **MTT-8**:319-325.
4. Gupta, K.C., Garg, R., and Chadha, R. (1981) *Computer Aided Design of Microwave Circuits*, Artech House, Dedham, MA.
5. McGrath, D.T., Mullinix, D.A., and Huck, K.D. (1986) *FORTRAN Subroutines for Design of Printed Circuit Antennas*, RADC-TM-86-08, ADB107263L.
6. Akhtarzad, S., Rowbotham, T.R., and Johns, P.B. (1975) The design of coupled microstrip lines, *IEEE Trans. Microwave Theory Tech.* **MTT-23:**486-492.
7. Kirschning, M. and Jansen, R.H. (1984) Accurate wide-range design equations for the frequency-dependent characteristics of parallel coupled microstrip lines, *IEEE Trans. Microwave Theory Tech.* **MTT-32**:83-90.
8. Butler, C.M. (1982) The equivalent radius of a narrow conducting strip, *IEEE Trans. Antennas Propag.* **AP-30:**755-758.
9. Balanis, C.A. (1982) *Antenna Theory*, Harper and Row, New York, pp. 319-321.

MISSION
of
Rome Air Development Center

RADC plans and executes research, development, test and selected acquisition programs in support of Command, Control, Communications and Intelligence (C^3I) activities. Technical and engineering support within areas of competence is provided to ESD Program Offices (POs) and other ESD elements to perform effective acquisition of C^3I systems. The areas of technical competence include communications, command and control, battle management, information processing, surveillance sensors, intelligence data collection and handling, solid state sciences, electromagnetics, and propagation, and electronic, maintainability, and compatibility.

Printed by
United States Air Force
Hanscom AFB, MA 01731